Effects of Spatial Variability and Scale on Areal-Average Evapotranspiration

J.S. FAMIGLIETTI and E.F. WOOD
Water Resources Program
Department of Civil Engineering and Operations Research
Princeton University
Princeton, New Jersey

Submitted to:
Water Resources Research
February 5, 1993

J. S. Famiglietti and E. F. Wood
Water Resources Program
Department of Civil Engineering and Operations Research
Princeton University
Princeton, New Jersey, 08544

ABSTRACT

This paper explores the effect of spatial variability and scale on areally-averaged evapotranspiration. A spatially-distributed water and energy balance model is employed to determine the effect of explicit patterns of model parameters and atmospheric forcing on modeled areally-averaged evapotranspiration over a range of increasing spatial scales. The analysis is performed from the local scale to the catchment scale. The study area is King's Creek catchment, an 11.7 km ^{2} watershed located on the native tallgrass prairie of Kansas. The dominant controls on the scaling behavior of catchment-average evapotranspiration are investigated by simulation, as is the existence of a threshold scale for evapotranspiration modeling, with implications for explicit versus statistical representation of important process controls. It appears that some of our findings are fairly general, and will therefore provide a framework for understanding the scaling behavior of areally-averaged evapotranspiration at the catchment and larger scales.

1. Introduction

The hydrologic cycle has a significant effect on land-atmosphere interaction over a range of scales. At the catchment or regional scale, this interaction determines the frequency of flooding and drought, as well as the quantity and quality of the water supply. At the grid scale of a general circulation model (GCM), the hydrology at the land surface determines important boundary conditions for climate simulations such as soil moisture and evapotranspiration. Globally, the distribution of atmospheric water has a major impact on climate, weather, and biogeochemical cycles. To better understand the role of hydrology in these interactions, improved land surface water and energy balance models are required, particularly at the larger scales.

Two of the major problems associated with the development of larger scale (catchment scale and greater) water and energy balance models are related to scaling and aggregation of hydrological processes. The scale problem addresses the relationship between spatial variability, scale, and the proper representation of hydrologic response at a particular scale. The second problem is related to aggregating process representations known at various space-time scales up to larger scales. What is the proper way to aggregate spatially-variable hydrologic processes whose dynamics occur at different space-time scales? Is the method of aggregation related to the scale of interest?

The second and third papers in this series investigated methods of aggregating a local water and energy balance model (Famiglietti and Wood, 1992a) up to larger scales. Famiglietti and Wood (1992b) presented a deterministic approach to spatial aggregation, utilizing digital elevation models (DEMs) and geographic information systems (GIS) to represent spatial variability explicitly. This model was proposed for use at the catchment scale due to the computational expense associated with applying the spatially-distributed model structure at larger scales. Famiglietti and Wood (1992c) utilized a statistical aggregation approach, in which the local model was aggregated with respect to a statistical distribution of a combined topographic-soils index (Beven, 1986). This model was proposed for use at larger scales with the implicit assumption that a statistical representation of actual patterns of topography, soils, and soil moisture is adequate to accurately model the water and energy fluxes at these scales, and that spatial variability in these variables dominates the spatial variability in the fluxes.

This paper investigates the validity of such assumptions by analyzing the relationship between spatial variability, spatial scale, areally-averaged evapotranspiration rates, and methods of aggregation. Specifically, we will explore the dynamics of areally-averaged evapotranspiration as spatial scale increases. For consistency with the previous papers in this series, the largest scale of application is the catchment scale. However, with adequate water and energy balance data, the analysis can be extended to much larger scales. The study area is the King's Creek catchment, an 11.7 km ^{2} watershed located on the native tallgrass prairie of Kansas. This area was the site of the First ISLSCP Field Experiment (FIFE) in 1987 and 1989 (Sellers et al., 1988). During FIFE, multiscale water and energy balance data were collected using ground-based and remote equipment. Thus the FIFE data afford unique opportunities to study the scaling behavior of hydrological processes.

The spatially-distributed water and energy balance model of Famiglietti and Wood (1992b) is used to explore the sensitivity of catchment-scale evapotranspiration rates to explicit patterns of model parameters and atmospheric forcing. Areally-averaged evapotranspiration computed with spatially-distributed fields of model parameters will be systematically compared to areally-averaged evapotranspiration computed with catchment-average parameter values. The analysis will be performed over a range of spatial scales, where increasing scale is represented by progressively larger subcatchments within the King's Creek catchment. We expect that at small scales, actual patterns of model parameters and inputs (e.g. root zone moisture content, soil properties, vegetation, solar radiation) are important factors governing catchment-scale evapotranspiration rates. However, as catchment scale increases, more of the variability in the distributions underlying these patterns is sampled. We suspect that at scales larger than some threshold scale, the mean evapotranspiration rate will no longer depend on the actual patterns of variability, but rather on the statistical characteristics representing the underlying distributions. Wood et al. (1988) termed this threshold scale a Representative Elementary Area (REA), analogous to the REV for porous media. They defined the REA as a "critical area at which continuum assumptions can be used without knowledge of the patterns of parameter values, although some knowledge of the underlying distributions may still be necessary." Using a simulation approach, they found that the REA exists at spatial scales on the order of 1 km ^{2} for catchment rainfall-runoff response.

In this study we wish to further analyze and probe the REA concept in the context of catchment-scale evapotranspiration. For evapotranspiration modeling, the existence of a

REA implies that at scales greater than the REA, exact patterns of spatially-variable model parameters and inputs need not be represented explicitly. However, it may still be necessary to account for the underlying variability of these parameters through distributional functions rather than representing an area in terms of uniform parameters.

In the next section an overview of the simulation analysis and a discussion of the simulation experiments is presented. The scope of the paper is then outlined, followed by a presentation of results, a discussion and summary of this work.

2. Overview of the Analysis

Wood et al. (1988) listed three requirements for this type of simulation experiment. First, a disaggregation scheme must exist for the study catchment so that it can be partitioned into a number of smaller subcatchments. Second, a local model of hydrologic processes must exist whose scale of application is much smaller than the smallest subcatchment, so that the average response of any subcatchment is equivalent to the average of the local responses within it. Third, spatially-distributed model inputs and parameters must exist so that the local model can be applied throughout the study catchment.

The first requirement is satisfied by the FIFE data set. A 30 m U. S. Geological Survey DEM is available for the King's Creek catchment area. Topographic analysis of the DEM yielded the 4 levels of discretization shown in Figure 1. The first level of disaggregation partitions the catchment into 66 subcatchments. The second level yields 39 subcatchments, the third 13, and the fourth 5 subcatchments.

The second requirement is satisfied by the spatially-distributed water and energy balance model. This model partitions the catchment into a number of 30 m grid elements which are coregistered with the local DEM and the FIFE GIS. The local water and energy balance model of Famiglietti and Wood (1992a) is applied at each grid element of the catchment.

The third requirement is also satisfied by the FIFE dat set. The local topographic-soils index was determined for each grid element in the catchment using the local DEM and FIFE GIS (see Famiglietti and Wood, 1992b). The various soils within the catchment were determined from the FIFE GIS and the corresponding soil parameters are given in Table 3 of Famiglietti and Wood (1992b). Some allowance for spatially-variable vegetation parameters was made in this study that was not made by Famiglietti and Wood (1992b). A 5 m tall vegetation was modeled along the stream channels (roughly 5 percent of the

catchment surface area). In these locations, the measurement height, z_a, was set equal to 7 m; the roughness length, z_0, was assumed equal to 0.8 m; the zero plane displacement, d, was assumed equal to 3.35 m; and a value of 5 x 10^9 s/m was assumed for R_u, the root resistance. Spatially-distributed clear-sky solar radiation was provided by Dubayah (personal communication) for the FIFE site for October 5, 1987. The remaining model parameters are summarized by Famiglietti and Wood (1992b) in Tables 1, 2, and 4 for FIFE intensive field campaign IFC4.

The spatially-distributed model was applied at the King's Creek catchment for the first 5 days of IFC4 (October 5-9, 1987). Simulations were run using the spatially-variable topographic, soil, moisture content, vegetation, and solar radiation data described above. Since this is primarily a sensitivity study and not a validation study, the spatially-distributed solar radiation data of October 5 were also used to force model simulations of October 6-9. Spatially-variable initial root and transmission zone moisture contents were also employed (see Figure 2). This simulation will be referred to as the control run in future sections. Additional simulations were run in which these spatially-distributed data were systematically held at catchment-average values. These simulations will be referred to as the sensitivity runs.

For a particular simulation, the local (grid-element) evapotranspiration fluxes were averaged over the various subcatchments shown in Figure 1 at selected times during the simulation. The average evapotranspiration rate for each of the subcatchments was plotted versus subcatchment area to analyze the effect of spatial variability on catchment-average evapotranspiration with increasing spatial scale. To determine the sensitivity of catchment-average evapotranspiration to spatial-variability in the various model parameters and inputs, plots of catchment-average evapotranspiration rate versus catchment area were compared for the control and sensitivity runs at different times during the simulations.

3. Scope of the Paper

This paper will focus on two sets of questions regarding the relationship between spatial heterogeneity, scale, and areally-averaged evapotranspiration:

1.) What is the effect of spatial heterogeneity on areally-averaged evapotranspiration rates as spatial scale increases? Does a REA exist for evapotranspiration modeling? This threshold scale would represent a fundamental building block for larger-scale evapotranspiration modeling. At scales larger than the REA it should be possible to simplify the representation of areally-averaged evapotranspiration response, while still retaining the important effects of heterogeneity in land-atmosphere interaction. For regions larger than the REA scale, actual patterns of important model variables such as soil moisture need not be considered; rather, their spatial variability can be considered statistically through their means and variances.

2.) To which spatially-variable model parameters is the scaling behavior of areally-averaged evapotranspiration most sensitive? (Note that the term 'scaling behavior' is defined here as the relationship between areally-averaged evapotranspiration rate and spatial scale.) Are there conditions under which evapotranspiration rates scale up? (The term 'scaling up' is defined here as an insignificant bias between evapotranspiration computed with spatially-variable versus spatially-constant model parameters and inputs.) These results will have important implications for modeling areally-averaged evapotranspiration at the catchment and larger scales. Relevant issues include which model parameters will require a statistical representation of spatial variability at scales greater than the REA scale, and which can be represented by simple areally-averaged or effective values.

As stated previously, this analysis was conducted for the King's Creek catchment at the FIFE site. The King's Creek catchment has little spatial variability in soil properties (predominantly silty clay loam), vegetation (predominantly native tallgrass) and topography (roughly 100 meters of elevation difference). Consequently, we expect spatial variability in root zone moisture content to be an important control on areally-averaged evapotranspiration rates. We expect this to be particularly true during periods of moisture stress, when evapotranspiration frequently occurs at soil or vegetation-controlled rates. Figure 3 shows the general form of the transpiration capacity-moisture content and exfiltration capacity-moisture content relationships used in the spatially-distributed model. These relationships

suggest that when soil and vegetation controls of evapotranspiration are active, and the spatial distribution of root zone moisture content includes the nonlinear portions of the curves, evapotranspiration will not scale up at King's Creek. Under these atmospheric and land surface conditions, we expect that a statistical representation of root zone moisture content will be required to adequately model evapotranspiration at spatial scales greater than the REA scale. In this study, we explore this hypothesis by simulating our control and sensitivity runs using data from FIFE IFC4, a period during which soil and vegetation-controls of evapotranspiration were active. The spatial distribution of initial root zone moisture content shown in Figure 2 was also employed in the simulations. This distribution yields significant spatial variability in transpiration and exfiltration capacities, so that the nonlinearity shown in Figure 3 is well represented within the catchment.

4. Results

Figure 4 shows simulated catchment-average evapotranspiration for the control run. To analyze the effect of spatial variability and scale on catchment-average evapotranspiration, the procedure outlined above was applied at numerous times during the simulation. The results for three times – 1245, 1415, and 1815 GMT, October 7, 1987 (0745, 0915 and 1315 local time; times 56, 57.5 and 61.5 in Figure 4) – are shown in Figure 5a. For comparison, Figure 5b shows catchment average evapotranspiration versus catchment area for a sensitivity run in which all model parameters and inputs were held at catchment-average values. Figure 5a shows that the effect of spatial variability has been in general, to increase the variability in the catchment-average evapotranspiration rate at small scales, and to increase the mean rate at all scales. Figure 5a suggests that a threshold (REA) scale does in fact exist which marks the transition from highly variable mean behavior at small scales, to stable mean behavior at larger scales. This figure also shows that the variability in the mean evapotranspiration rate at small scales, and thus the REA scale, is greater at mid-day than in the morning. It is inferred that for areas larger than the REA, most of the variability in model parameters and inputs has been sampled, so that at larger scales, the mean evapotranspiration rate stabilizes.

Note that the times shown in Figure 5 should be considered representative time steps for the simulation. Similar scaling behavior was observed throughout the simulation at the

corresponding times each day (i.e. an increase in the REA scale from local scales in the morning to 1 - 2 km ^{2} at mid-day, and decreasing back to local scales in the late afternoon).

The significant bias between evapotranspiration computed with and without spatially-variable model parameters indicates that spatial heterogeneity in land surface-atmosphere interaction plays a major role in the simulation of catchment-average evapotranspiration. To elucidate fundamental relationships between spatial variability, scale, and evapotranspiration fluxes, the scaling analysis described above was applied to the three components of simulated evapotranspiration – evaporation from the wet canopy, transpiration from the dry canopy, and evaporation from bare soils – at the same times as in Figure 5. In each case an attempt was made to determine the spatially-variable model parameters to which the component was most sensitive, and whether this sensitivity changed diurnally. This analysis should result in a better understanding of the important process controls on areally-averaged evapotranspiration, and thus the scaling behavior shown in Figure 5a, with implications for how these controls should be represented within land surface parameterizations.

The results of the scaling analysis are described in detail for bare soil evaporation, since evaporation from bare soils was the primary component of evapotranspiration during FIFE IFC4 due to senescence of the native tallgrass (see Figure 6). The results for wet canopy evaporation and dry canopy transpiration are analogous to those for bare soil evaporation. These results are presented in detail by Famiglietti (1992) and are only briefly described here.

4.1 Bare-Soil Evaporation

The actual rate of evaporation from bare soils, e_{bs}, is given by Famiglietti and Wood (1992b) as

$$e^i_{bs} = min[e^{*i}, e^i_{pe}] \tag{1}$$

where i is the grid element index, e^* is the local exfiltration capacity and e_{pe} is the local potential evaporation rate. When the exfiltration capacity is less than the potential evaporation rate, the actual evaporation rate is equal to the exfiltration capacity. Evaporation under these conditions is known as soil-controlled evaporation. In this section the scaling behavior of bare-soil evaporation is investigated in terms of its two components, the exfiltration capacity and the potential evaporation.

4.1.1 *Potential Evaporation*

Figure 7 shows the computed catchment-average potential evaporation rate versus catchment scale for the three representative time steps during the control simulation (1245, 1415, and 1815 GMT, October 7, 1987). In each case, the catchment-average potential evaporation shows more variability at small scales than at large scales. Figure 7 suggests that a threshold (REA) scale exists which marks this transition in mean behavior. This figure also shows that the variability in catchment average potential evaporation at small scales, and thus the REA scale, is greater at mid-day than in the morning.

To better understand the sources of variation in computed catchment-average potential evaporation with scale, two sensitivity runs were simulated. Of the parameters assumed spatially variable in this report, those that affect potential evaporation most significantly are solar radiation and soil properties. The two sensitivity runs utilized the following combinations of model inputs: spatially-constant solar radiation and spatially-constant soil properties (crcs); and spatially-constant solar radiation and spatially-variable soil properties (crvs). These were compared to the control run, which was generated with spatially-variable solar radiation data and spatially-variable soil properties (vrvs). Spatially-constant model inputs were held at their catchment-average values.

Figure 8 shows computed catchment-average potential evaporation rates versus catchment scale at 1815 GMT for the control and sensitivity runs. The solid line represents catchment-average potential evaporation for the case of spatially-constant solar radiation and soil properties. The inclusion of spatially-variable soil properties has a minor effect on catchment-average potential evaporation rates at all scales. The inclusion of spatially-variable solar radiation has a significant impact on the catchment-average potential evaporation, yielding a high degree of variability at small scales. At larger scales however, spatial variability in solar radiation has less of an effect on catchment-average potential evaporation rates. Figure 8 also shows that the REA scale for the potential evaporation rate at this time is 1.0 - 2.0 km ^{2}. We believe that at this scale, most of the spatial variability in the solar radiation has been sampled, so that at larger scales the mean potential evaporation rate stabilizes.

4.1.2 *Exfiltration Capacity*

To better understand the scaling behavior of catchment-average exfiltration capacity, three sensitivity runs were simulated and compared to the control run (vmvrvs). Of the

parameters that are assumed spatially variable in this work, those with the most significant impact on exfiltration capacities include root zone moisture content, soil properties, and solar radiation. We systematically held these parameters at their catchment-average values in the sensitivity runs. In the first simulation, spatially-constant soil moisture, solar radiation and soil properties were employed (cmcrcs). The second simulation maintained constant solar radiation and soil properties, but was initialized with the spatial distribution of root zone moisture content shown in Figure 2 (vmcrcs). The third simulation added spatially-variable soil properties to the list of model inputs used in the second simulation (vmcrvs).

Figure 9 shows catchment-average exfiltration capacity versus catchment scale at 1815 GMT, October 7, 1987, for the control and sensitivity runs described above. The lower line (cmcrcs) represents catchment-average exfiltration capacity for spatially-constant soil moisture, solar radiation and soil properties. The upper line (vmcrcs) shows the impact of including spatially-variable moisture content to the simulation. The mean exfiltration capacity has increased over all scales, and its variability has increased significantly at small scales. The inclusion of spatially-variable soil properties has lowered the mean exfiltration capacity over all scales. The inclusion of spatially-variable solar radiation has little impact on the mean exfiltration capacity over all scales. Figure 9 implies that, for the parameter combinations tested, the dominant control on the scaling behavior of the catchment-average exfiltration capacity is the spatial distribution of moisture content. Figure 9 also shows that the REA scale for exfiltration capacity at this time step is roughly 1.0 - 2.0 km ^{2}. At this scale, most of the spatial variability in the moisture content, solar radiation and soil properties has been sampled, so that at larger scales the mean exfiltration capacity stabilizes.

These results are best understood by considering the relationship of the spatial distribution of root zone moisture content (see Figures 2 for the distribution used to initialize the simulations) to the exfiltration capacity - soil moisture relationship shown in Figure 3. When the moisture content distribution lies on a linear portion of this curve, spatial variability in moisture content has little effect on the catchment-average exfiltration capacity. However, when the moisture content distribution includes the nonlinear portion of the curve, spatial variability in moisture content has a significant impact on the catchment-average exfiltration capacity.

4.1.3 Actual Bare-Soil Evaporation

The effect of including spatially-variable soil moisture and other model inputs in a spatially-distributed catchment simulation is that different catchment locations evaporate

at different rates during the same time step. At any time, all bare-soil locations within the catchment fall into two groups – those evaporating at the potential rate and those evaporating at soil-controlled exfiltration capacities. Thus, variability in the catchment-average actual evaporation rate with scale is a function of the relative amounts of land surface evaporating at potential or soil-controlled rates and the scaling behavior of these two components. (See Famiglietti and Wood (1992c), who compute the amount of land surface evaporating at potential or soil-controlled rates for each time step during IFC4). If the REA scale differs for the potential and capacity components of evaporation, then the REA scale for the actual evaporation rate should vary according to the amount of land surface evaporating under either condition. To explore these interactions, actual bare-soil evaporation was computed for the first five days of IFC4 for the control run. The catchment-average potential evaporation rate, exfiltration capacity, and actual evaporation rate were plotted versus catchment scale for 1245, 1415, and 1815 GMT, October 7, 1987.

Figure 10a shows the results at 1245 GMT. In the early morning, the potential evaporation rate is low, as shown by the lower line, and the simulation results indicates that most of the catchment evaporates at this low rate. The catchment-average actual evaporation rate should nearly equal the catchment-average rate of potential evaporation. Figure 10a shows that in fact the two are essentially equal. In the morning, when most of the catchment is evaporating at the potential rate, the dominant controls on the scaling behavior of the catchment-average actual evaporation rate (and thus its REA) are those associated with the potential evaporation rate.

Figure 10b presents the results for 1415 GMT (mid-morning). As the potential evaporation rate increases (middle line), more of the catchment evaporates at soil-controlled rates. Thus, the degree of variability in the catchment-average actual evaporation (lower line) at small scales is greater than that of the potential evaporation, but less than that of the exfiltration capacity. Both the potential and capacity components are contributing to the variability in catchment-average actual evaporation at small scales, and to the mean actual evaporation rate over all scales.

The results for 1815 GMT (mid-day) are displayed in Figure 10c. At mid-day, the potential evaporation rate (middle line) exceeds the exfiltration capacity (upper line) over much of the catchment. Thus the catchment-average actual evaporation rate reflects more of the variability of the catchment-average exfiltration capacity. More bare-soil locations within the catchment have switched from evaporation at potential rates to soil-controlled

rates. Consequently, the dominant controls of the scaling behavior of catchment-average actual evaporation have switched from those associated with the potential evaporation rate to those associated with the exfiltration capacity.

Figure 11 shows the catchment-average actual evaporation rate versus catchment scale for 1245, 1415, and 1815 GMT. This figure clearly shows the increase in variability of the catchment-average actual evaporation rate at small scales with time. Figure 11 also suggests that the REA scale increases with time, from very small scales in the morning, to 1.0 - 2.0 km ^{2} at mid-day. Both the increased variability at small scales and the increase in the REA scale reflect the change in evaporation modes within the catchment, from predominantly potential rates in the morning, to predominantly soil-controlled rates at mid-day.

4.2 Dry Canopy Transpiration and Wet Canopy Evaporation

Famiglietti (1992) observed scaling behavior similar to that of bare soil evaporation for the cases of dry canopy transpiration and wet canopy evaporation. As in the case of bare-soil evaporation, an increase in the REA scale was noted, from local scales in the early morning to 1.0 - 2.0 km ^{2} at mid-day. Figure 12 shows these dynamics for the catchment-average actual transpiration rate. Both the increased variability at small scales and the increase in the REA scale correspond to the change of transpiration modes within the catchment, from primarily unstressed rates in the morning, to predominantly vegetation-controlled rates at mid-day. As the mechanisms of transpiration switch from those associated with unstressed rates to those associated with increased stomatal control, the dominant controls on the scaling behavior of catchment-scale transpiration switch accordingly. The dominant spatially-variable model parameters for the various components of evapotranspiration are summarized in Table 1 for the King's Creek catchment during FIFE IFC4.

4.3 Evapotranspiration

Famiglietti and Wood (1992a) compute local rate of evapotranspiration, e^i, as

$$e^i = f^i_{bs} e^i_{bs} + f^i_v [e^i_{wc} + e^i_{dc}] \tag{2}$$

where f_{bs} is the local fraction of bare soil, f_v is the local fraction of vegetated soil, e_{wc} is rate of evaporation from the wet canopy, and e_{dc} is rate of transpiration from the dry canopy. The

catchment-average evapotranspiration rate is simply the average of the local rates, or the sum of the average bare-soil, wet canopy, and dry canopy components of evapotranspiration.

Figure 13 shows the catchment-average evapotranspiration rate versus catchment scale at 1415 GMT, October 7, 1987. The catchment-average bare-soil, dry canopy and wet canopy evaporation components are plotted as well. The weighted sum of these components yields the catchment-average evapotranspiration rate at any scale. The variability in the catchment-average evapotranspiration rate with scale is therefore a function of the variability of its components.

The catchment-average evapotranspiration rate versus catchment scale is shown in Figure 5a for 1245, 1415, and 1815 GMT, October 7, 1987. The scaling behavior of catchment-average evaptranspiration reflects that of its components, described above. The variability at small scales increases with time until mid-day. The REA scale shows a corresponding increase with time, from small scales in the morning, to 1.0 - 2.0 km ^{2} at mid-day. Both the increased variability at small scales and the increase in the REA scale reflect the change in the dominant controls on the catchment-average evapotranspiration rate, from those associated with potential rates in the morning, to those associated with soil and vegetation-controlled rates at mid-day.

5. Discussion

5.1 Effects of Spatial Variability and Scale on Areal-Average Evapotranspiration

The previous sections have shown that for the simulations conducted in this study, the dominant controls on the scaling behavior of catchment-average evapotranspiration depend on the dominant controls on its components – evaporation from the wet canopy, transpiration from the dry canopy, and evaporation from bare soils. The controls on these components depend in turn on whether evapotranspiration is occurring at potential rates or soil and vegetation-controlled rates.

In general, when root-zone moisture content levels are relatively high, or the potential evapotranspiration rates are low, evapotranspiration will occur at predominantly potential rates. The scaling behavior of catchment-average evapotranspiration under these conditions is largely determined by the controls on the potential evapotranspiration rates. When

root zone moisture content levels are low, or potential evapotranspiration rates are high, evapotranpiration will occur at soil and vegetation-controlled rates. The scaling behavior of catchment-average evapotranspiration is dominated by the controls on the soil and vegetation-controlled rates.

The interaction between the land surface and the atmosphere will have both seasonal and diurnal time scales. For example, during wetter periods, evapotranspiration will occur at predominantly potentential rates. However, the space-time variability in atmospheric forcing and moisture content, as well as the spatial variability in vegetation and soils, will result in portions of the catchment evaporating at soil or vegetation-controlled rates if the potential evapotranspiration rate is too high (e.g. at mid-day), or if moisture content levels fall too low (e.g. during an extended interstorm period). Conversely, during dry periods, more evapotranspiration will occur at moisture-stressed rates, but some or all of the catchment may evaporate at potential rates when the potential rates are low (e.g. in the early morning), or if root zone moisture contents rise to high levels (e.g. after a storm). The seasonal and diurnal dynamics of land-atmosphere interaction will be reflected in the scaling behavior of catchment-average evapotranspiration.

5.2 Implications for Hydrologic Modeling

This study outlines a methodology for assessing the importance of spatial variability in land surface and atmospheric variables for modeling evapotranspiration at the catchment scale. The existence of an REA scale for simulated evaptranspiration indicates how spatial variability in important variables can be incorporated into hydrological models. At scales greater than the REA scale, much of the variability in the underlying distributions of land surface parameters and atmospheric forcing has been sampled. At these scales, a statistical representation of spatial variability in important model parameters and inputs is adequate for evapotranspiration modeling (i.e. a statistically-aggregated model of land hydrologic processes is an appropriate representation for catchment evapotranspiration modeling). At scales less than the REA scale, explicit patterns of important spatially-variable model parameters and inputs have a significant impact on simulated evapotranspiration. At these scales a spatially-explicit aggregation approach is required to model catchment-average evapotranspiration at scales less than the REA scale.

One example of a statistical aggregation procedure is given by Famiglietti and Wood (1992c). They present a statistical-dynamical hydrological model, in which the local water

and energy balance model is aggregated with respect to a probability density function of combined topographic and soil properties. The spatial variability in topographic and soil properties results in spatial variability in modeled moisture content and the water and energy fluxes related to moisture content, such as runoff and evapotranspiration. All other model parameters and inputs in the statistical model are represented by catchment-average values. However, when spatial variability in these other parameters is correlated to the spatial distribution of the topographic-soils index (e.g. vegetation parameters), it can easily be incorporated into the model framework.

Figure 14 compares catchment-average evapotranspiration computed for the King's Creek catchment (for October 5-9, 1987) using the spatially-distributed model, the statistically-aggregated model, and the one-dimensional local model. The middle line in Figure 14 represents the control simulation of evapotranspiration computed using the spatially-distributed model with all model inputs and parameters varying spatially. The upper line represents evapotranspiration computed with the statistically-aggregated model. The difference between these two simulations results from the combined effect of representing spatially-variable moisture content statistically and all other model inputs and parameters with catchment-average values (e.g. solar radiation, vegetation, soil properties). The lower line represents evapotranspiration computed with the one-dimensional model. The one-dimensional simulation represents the effect of holding all model inputs and parameters, including initial root zone moisture content and the topography, at catchment-average values. At the catchment scale there is little difference between explicitly and statistically- aggregated evapotranspiration at the King's Creek catchment. However, there is a significant difference between the simulations run with spatially-constant and spatially-variable initial root zone moisture content.

Figure 14 clearly indicates that at the King's Creek catchment, during IFC4, a period when soil and vegetation controls of evapotranspiration were active, modeled evapotranspiration does not scale up during mid-day hours. The considerable bias between evapotranspiration computed with spatially-variable root zone moisture content and catchment-average moisture content indicates further that some representation of spatial variability in root zone moisture content (and in this case, the topographic-soil index, which is employed to model topographic redistribution of subsurface soil moisture and thus spatial variability in root zone moisture content) more so than other model parameters, is required for realistic simulation of evapotranspiration during this time period. Figure 14 also shows that at the scale of the

King's Creek catchment, which is greater than the REA scale, a statistical representation of the spatial variability in topography, and thus root zone moisture content, is an adequate representation of the actual patterns represented within the spatially-distributed model.

As previously mentioned, our choice to simulate evapotranspiration during IFC4 at the King's Creek catchment was made to investigate the role of spatial variability in root zone moisture content. Consequently, these results may be in part site, model, and time dependent. For example, a site with greater spatial variability in vegetation may show a stronger dependence on vegetation parameters than root zone soil moisture content. Or, if the comparison shown in Figure 14 were repeated during IFC3 (August 6-21, 1987), a period during which root zone moisture content was relatively wet and evapotranspiration occurred at potential rates, then spatial variability in moisture content may not be the dominant control on the scaling behavior of areally-averaged evapotranspiration. Under these land and atmospheric conditions, evapotranspiration may scale up more readily. Similarly, we suggest that later in the year, or in general when the spatial distribution of root zone moisture content is relatively dry with little spatial variability, even though evapotranspiration may occur under active soil and vegetation control, it may again scale up readily.

However, we believe that the findings presented here provide a framework for understanding and modeling areally-averaged evapotranspiration at the catchment and larger scales. The concept that the dominant controls on areally-averaged evapotranspiration vary with the amount of land surface evaporating at potential rates versus soil or vegetation-controlled rates, is, we propose, site independent and applicable at larger scales. At these larger scales ($O(10000\ km^2)$), the variability in the various components of areally-averaged evapotranspiration may be a function of large scale controls that are not evident at the catchment scale. For example, topographic, soil, and vegetation properties may vary on the scale of regional geology and climate. Soil moisture may vary on the scale of storm systems. Potential evapotranspiration may vary with synoptic-scale weather patterns and variations in vegetation and soil properties. The behavior of areally-averaged evapotranspiration from the catchment scale to the scale of a GCM grid square, and the land surface-atmosphere conditions under which evapotranspiration will scale up, are the subjects of ongoing research.

6. Summary

In this paper we explored the effect of spatial variability and scale on areally-averaged evapotranspiration. We employed a spatially-distributed model to determine the effect of explicit patterns of model parameters and atmospheric forcing on modeled areally-averaged evapotranspiration over a range of increasing spatial scales, from the local scale to the catchment scale. The study catchment was the King's Creek catchment, an 11.7 km ^{2} watershed located on the native tallgrass prairie of Kansas.

This report shows that an REA scale exists for catchment-scale evapotranspiration modeling at the King's Creek catchment. We believe that at scales greater than this threshold scale, a statistically-aggregated model of land hydrologic processes is an appropriate representation for catchment evapotranspiration modeling. At scales less than the REA scale, we believe that a spatially-explicit aggregation approach is required to model catchment-average evapotranspiration.

The simulations conducted for the King's Creek catchment showed that the dominant controls on the scaling behavior of catchment-average evapotranspiration depend on the dominant controls on its components – evaporation from the wet canopy, transpiration from the dry canopy, and evaporation from bare soils. The controls on these components depend in turn on whether evapotranspiration is occurring at potential rates or soil and vegetation-controlled rates. During FIFE IFC4, a period of significant soil and vegetation control of evapotranspiration, spatial variability in root zone moisture content was shown to be the dominant control on areally-averaged evapotranspiration for the catchment. It was shown by example that some representation of spatial variability in root zone moisture content was required to avoid significant bias in computed evapotranspiration during IFC4. It was also shown that a statistical representation of this spatial variability was adequate at the catchment scale.

Although this work was performed for a specific location at the catchment scale, we believe that the some of the concepts outlined here are fairly general. Therefore, we believe that these findings will provide a framework for understanding the scaling behavior of areally-averaged evapotranspiration at the catchment and larger scales.

Acknowledgements. This work was supported by NASA grants NAGW-1392 and NGT-

60153; this research support is gratefully acknowledged. We thank Ralph Dubayah for providing spatially-distributed solar radiation data for the FIFE site. We thank Dominique Thongs for providing the spatial averaging software and for his help in processing other spatially-distributed FIFE data. This work benefited greatly from discussions with Robert Gurney.

TABLE 1. Dominant Spatially-Variable Model Parameters

	wet canopy evaporation	dry canopy transpiration	bare soil evaporation
potential/unstressed rates	vegetation	vegetation	-
soil/vegetation controlled rates	-	root zone moisture content	root zone moisture content

7. References

1. BEVEN, K., 1986: Runoff production and flood frequency in catchments of order n: An alternative approach. *Scale problems in hydrology*, V. K. Gupta et al. Eds., D. Reidel Publishing Company, 107-131.
2. BROOKS, R. H. AND A. T. COREY, 1964: Hydraulic properties of porous media. *Hydrology Paper No. 3*, Colorado State Univ., Ft. Collins, Colorado.
3. FAMIGLIETTI, J. S., 1992: Aggregation and scaling of spatially-variable hydrological processes: Local, Catchment-Scale, and Macroscale Models of Water and Energy Balance. Ph. D. dissertation, Department of Civil Engineering and Operations Research, Princeton University, Princeton, NJ.
4. FAMIGLIETTI, J. S. AND E. F. WOOD, 1992a: Aggregation and scaling of spatially-variable hydrological processes, 1, A local model of water and energy balance. Submitted to
5. FAMIGLIETTI, J. S. AND E. F. WOOD, 1992b: Aggregation and scaling of spatially-variable hydrological processes, 2, A catchment-scale model of water and energy balance. Submitted to *Wat. Resour. Res.*
6. FAMIGLIETTI, J. S. AND E. F. WOOD, 1992c: Aggregation and scaling of spatially-variable hydrological processes, 3, A macroscale model of water and energy balance. Submitted to *Wat. Resour. Res.*
7. SELLERS, P. J., F. G. HALL, G. ASRAR, D. E. STREBEL, AND R. E. MURPHY, 1988: The first ISLSCP field experiment (FIFE). *Bull. Amer. Meteor. Soc.*, **69**, 22-27.
8. SIVAPALAN, M., K. BEVEN AND E. F. WOOD, 1987: On hydrologic similarity, 2. A scaled model of storm runoff production. *Water Resour. Res.* **23**, 2266-2278.
9. WOOD, E. F., M. SIVAPALAN, K. BEVEN, AND L. BAND, 1988: Effects of spatial variability and scale with implications to hydrologic modeling. *J. Hydrol.* **102**, 29-47.

Figure Captions List

Fig. 1. Disaggregation of the King's Creek catchment into subcatchments. From left to right and top to bottom: 66, 39, 13, and 5 subcatchments.

Fig. 2. Spatial distribution of root zone moisture content used to initialize simulations of IFC4. The scale black to white represents 45 percent by volume to less than 10 percent by volume.

Fig. 3. General form of transpiration capacity and exfiltration capacity versus moisture content utilized in Famiglietti and Wood (1992a).

Fig. 4. Evapotranspiration computed for the King's Creek catchment during FIFE IFC4, October 5-9, 1987 (control run). Time 0 corresponds to 445 GMT, October 5.

Fig. 5. Computed catchment-average evapotranspiration rate versus catchment area for 1245, 1415, and 1815 GMT, October 7, 1987: a.) control run; b.) all parameters spatially-averaged.

Fig. 6. Evapotranspiration computed for the King's Creek catchment during FIFE IFC4, October 5-9, 1987 (control run): a.) for bare soil (ebs), dry canopy (edc), and wet canopy (ewc) components, and total evapotranspiration (et); b.) for each component weighted by the fraction of bare soil (fbs) or the fraction of vegetated surface (fv). Time 0 corresponds to 445 GMT, October 5.

Fig. 7. Computed catchment-average potential evaporation versus catchment area for three 1245, 1415, and 1815 GMT, October 7, 1987.

Fig. 8. Computed catchment-average potential evaporation versus catchment area at 1815 GMT, October 7, 1987 for spatially-constant solar radiation and spatially-constant soil properties (crcs); spatially-constant solar radiation and spatially-variable soil properties (crvs); and spatially-variable solar radiation and spatially-variable soil properties (vrvs).

Fig. 9. Computed catchment-average exfiltration capacity versus catchment area at 1815 GMT, October 7, 1987 for the following combinations of model inputs: spatially-constant moisture content, solar radiation, and soil properties (cmcrcs); spatially-variable moisture content and spatially-constant solar radiation and soil properties (vmcrcs); spatially-variable soil moisture and soil properties and spatially-constant solar radiation (vmcrvs); spatially-variable moisture content, solar radiation and soil properties (vmvrvs).

Fig. 10. Computed catchment-average potential evaporation, exfiltration capacity, and actual evaporation versus catchment area for October 7, 1987: a.) 1245 GMT; b.) 1415 GMT; and c.) 1815 GMT.

Fig. 11. Computed catchment-average actual evaporation rate versus catchment area for 1245, 1415, and 1815 GMT, October 7, 1987.

Fig. 12. Computed catchment-average actual transpiration rate versus catchment area for 1245, 1415, and 1815 GMT, October 7, 1987.

Fig. 13. Computed catchment-average evapotranspiration rate, catchment-average wet canopy evaporation rate, catchment-average dry canopy transpiration rate, and catchment-average bare soil evaporation rate versus catchment area for 1415 GMT, October 7, 1987.

Fig. 24. Computed catchment-average evapotranspiration using the spatially-distributed model (explicit), the statistically-aggregated model (statistical), and the one-dimensional local model (1-d), October 5-9, 1987.

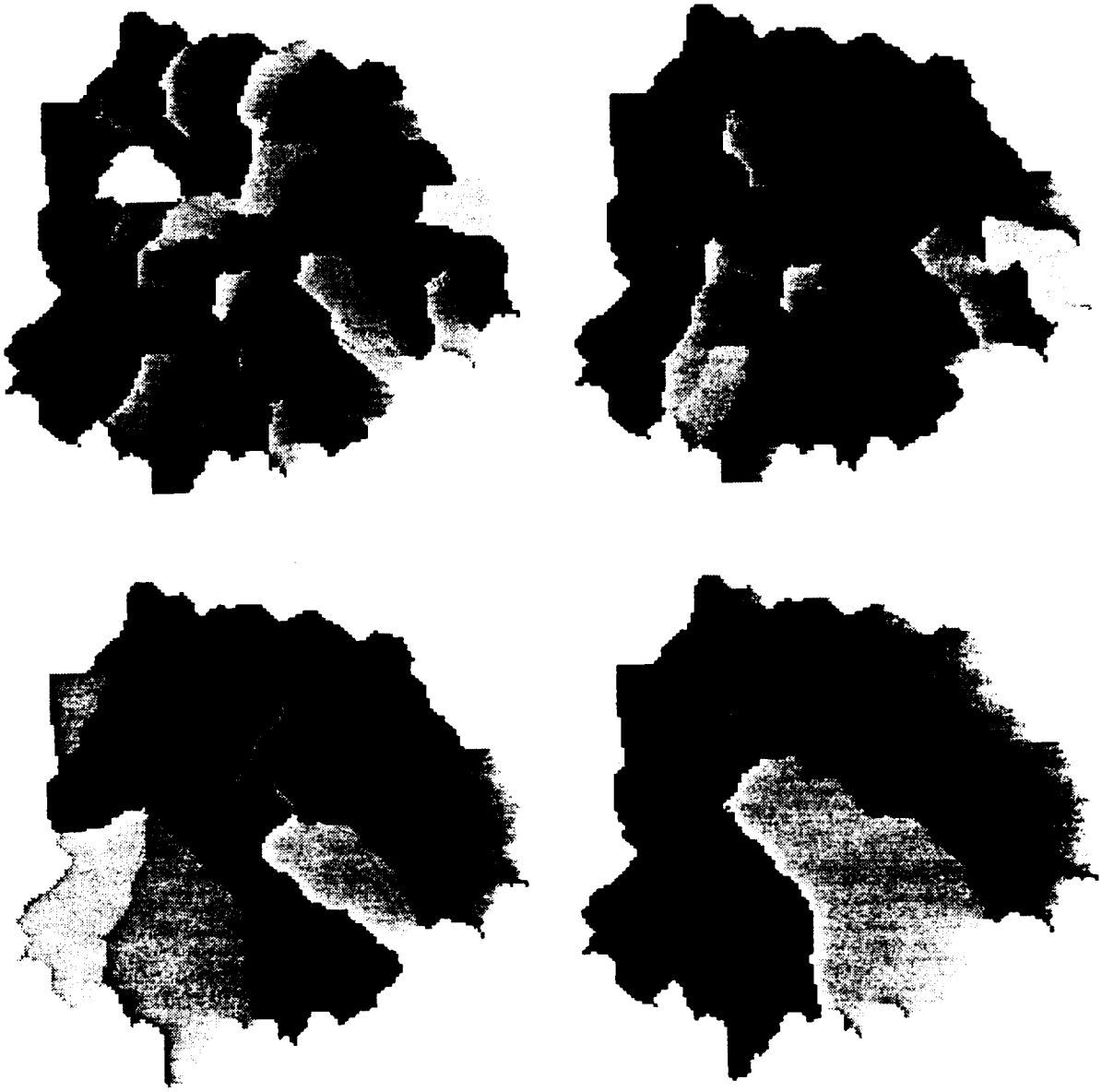

Figure 1. Disaggregation of the King's Creek catchment into subcatchments. From left to right and top to bottom: 66, 39, 13, and 5 subcatchments.

Figure 2. Spatial distribution of root zone moisture content used to initialize simulations of IFC4. The scale black to white represents greater thean 45 percent by volume to less than 10 percent by volume.

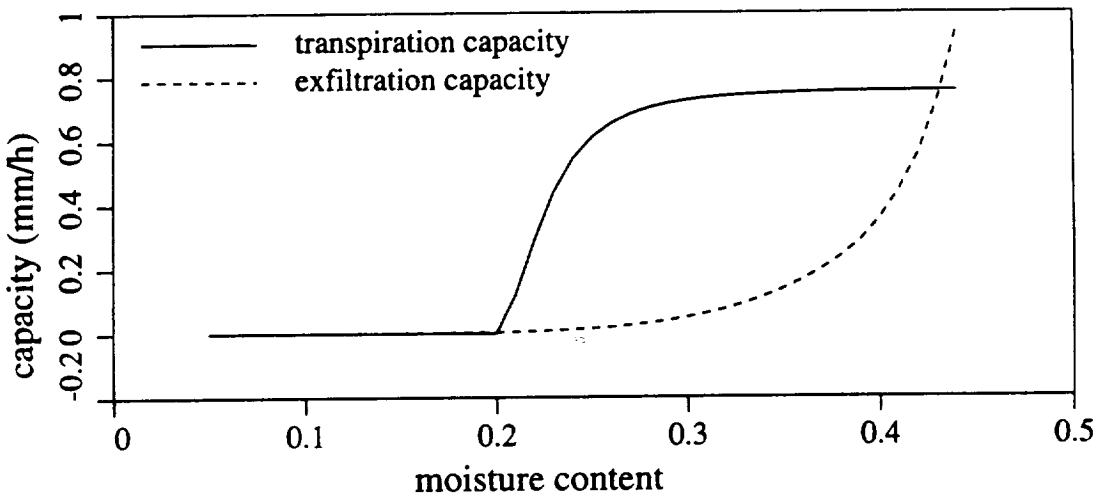

Figure 3. General form of transpiration capacity and exfiltration capacity versus moisture content utilized in Famiglietti and Wood (1992a-c).

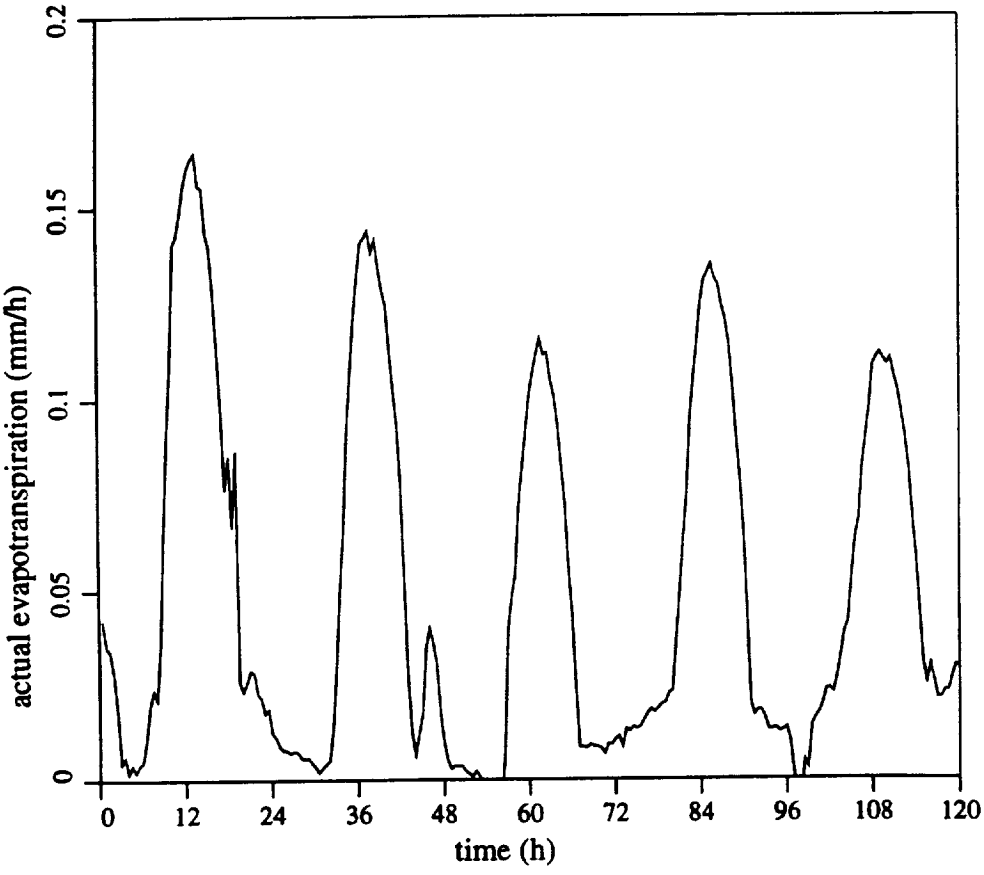

Figure 4. Evapotranspiration computed for the King's Creek catchment during FIFE IFC4, October 5-9, 1987 (control run). Time 0 corresponds to 445 GMT, October 5.

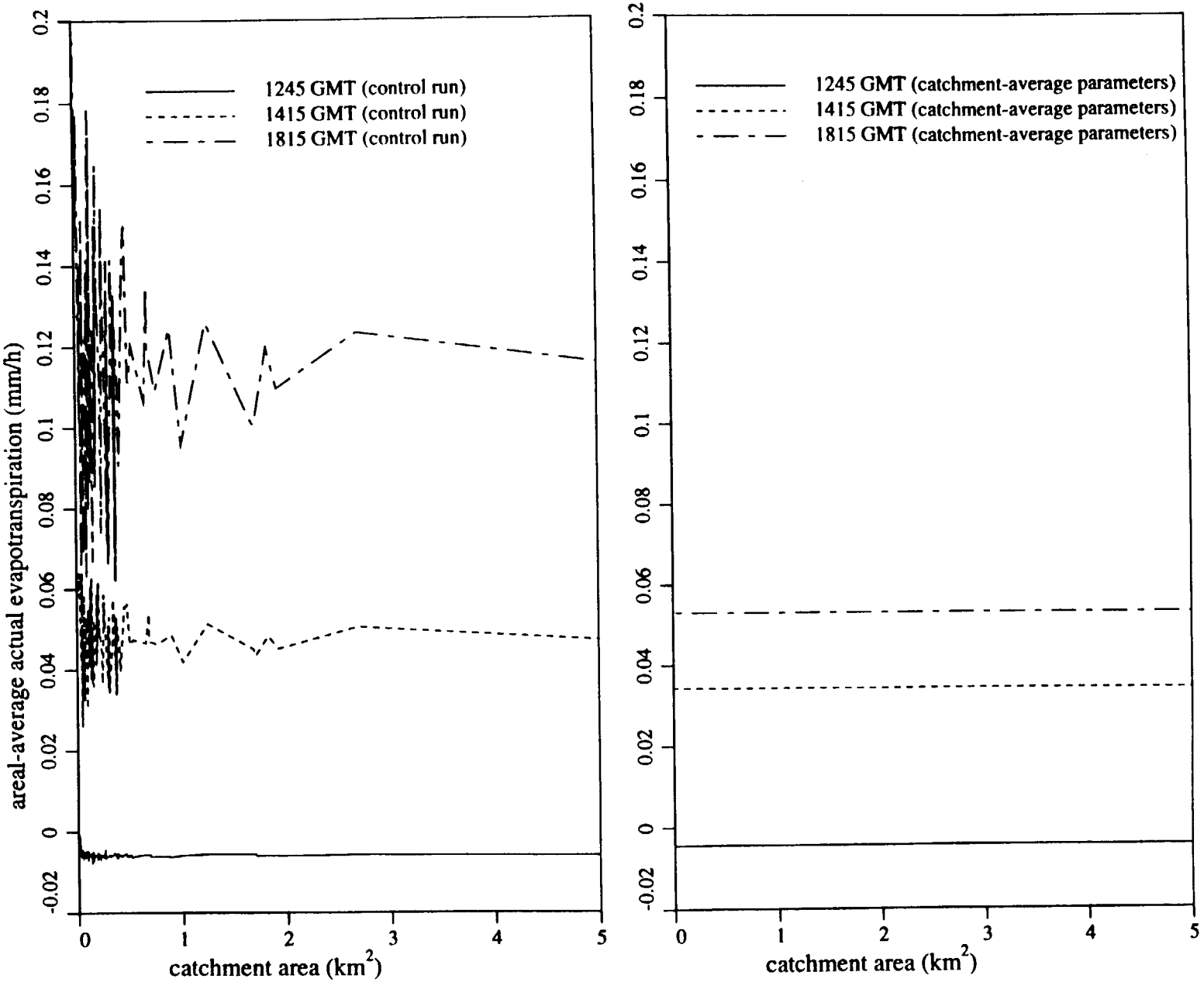
areal-average actual evapotranspiration (mm/h)
0.2
0.18
0.16
0.14
0.12
0.1
0.08
0.06
0.04
0.02
0
-0.02
1245 GMT (control run)
1415 GMT (control run)
1815 GMT (control run)
0
1
2
3
4
5
catchment area (km^2)
1245 GMT (catchment-average parameters)
1415 GMT (catchment-average parameters)
1815 GMT (catchment-average parameters)
catchment area (km^2)

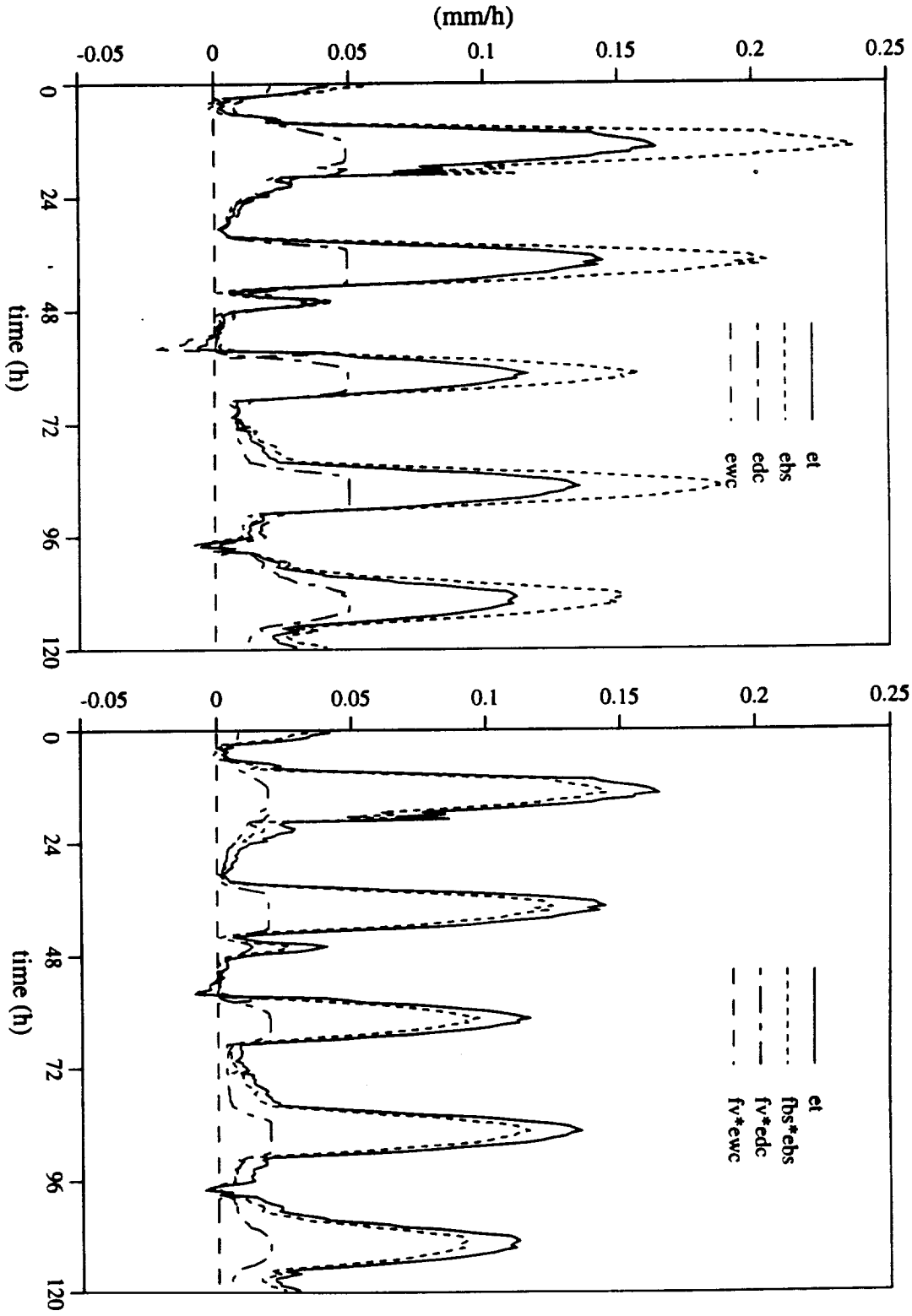
(mm/h)
-0.05
0
0.05
0.1
0.15
0.2
0.25
time (h)
0
24
48
72
96
120
et
ebs
edc
ewc
et
fbs*ebs
fv*edc
fv*ewc

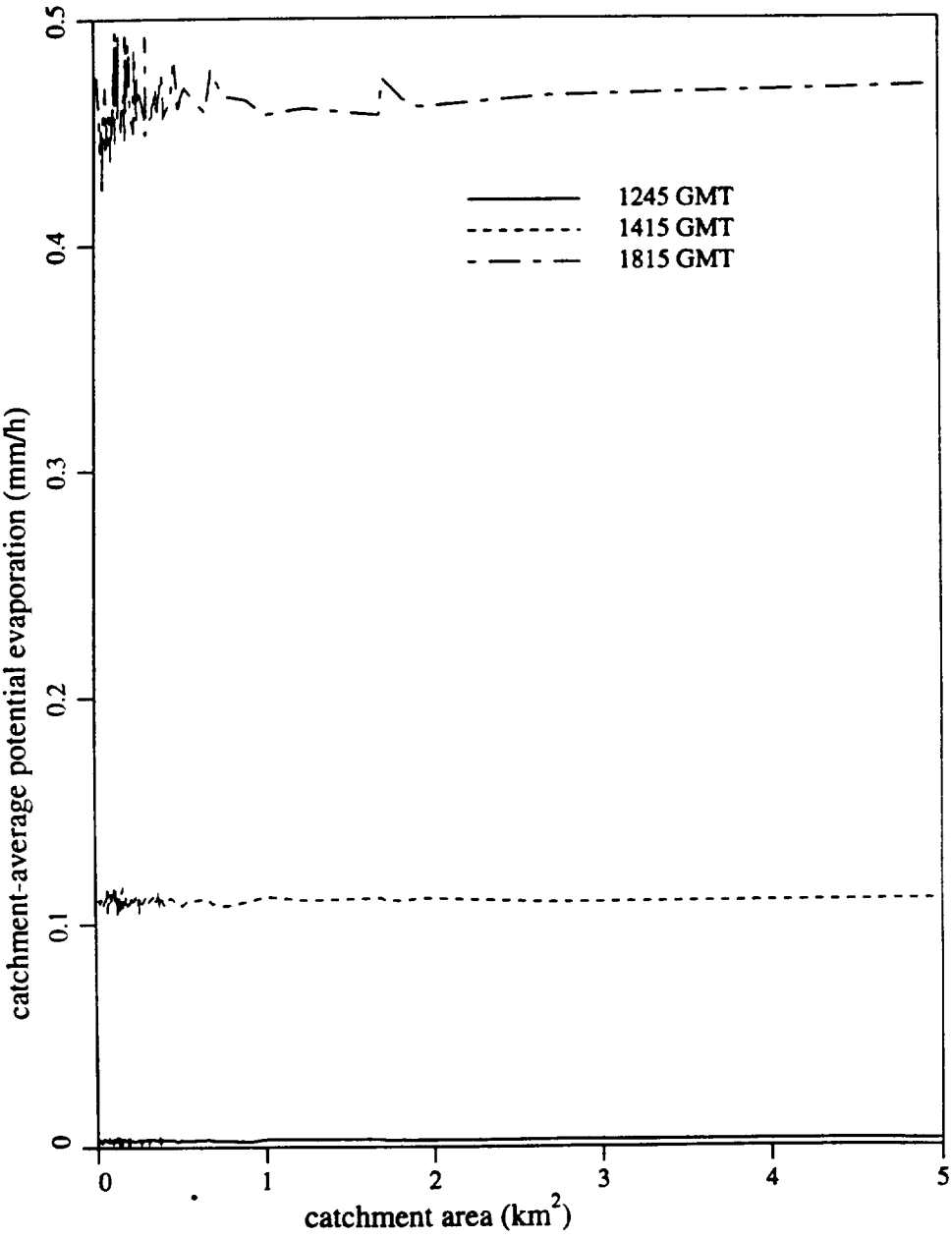

Figure 7. Computed catchment-average potential evaporation versus catchment area for three 1245, 1415, and 1815 GMT, October 7, 1987.

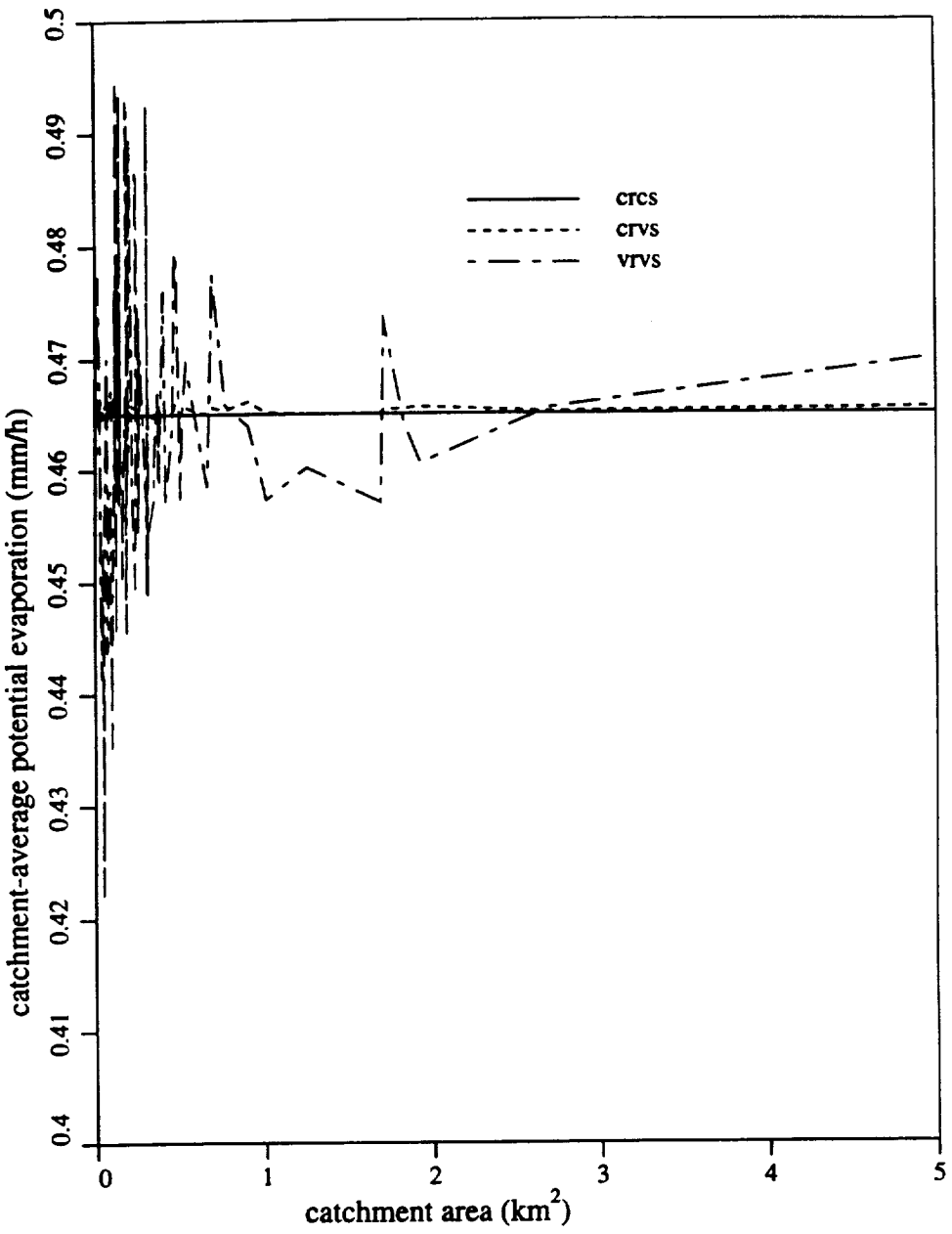

Figure 8. Computed catchment-average potential evaporation versus catchment area at 1815 GMT, October 7, 1987 for spatially-constant solar radiation and spatially-constant soil properties (crcs); spatially-constant solar radiation and spatially-variable soil properties (crvs); and spatially-variable solar radiation and spatially-variable soil properties (vrvs).

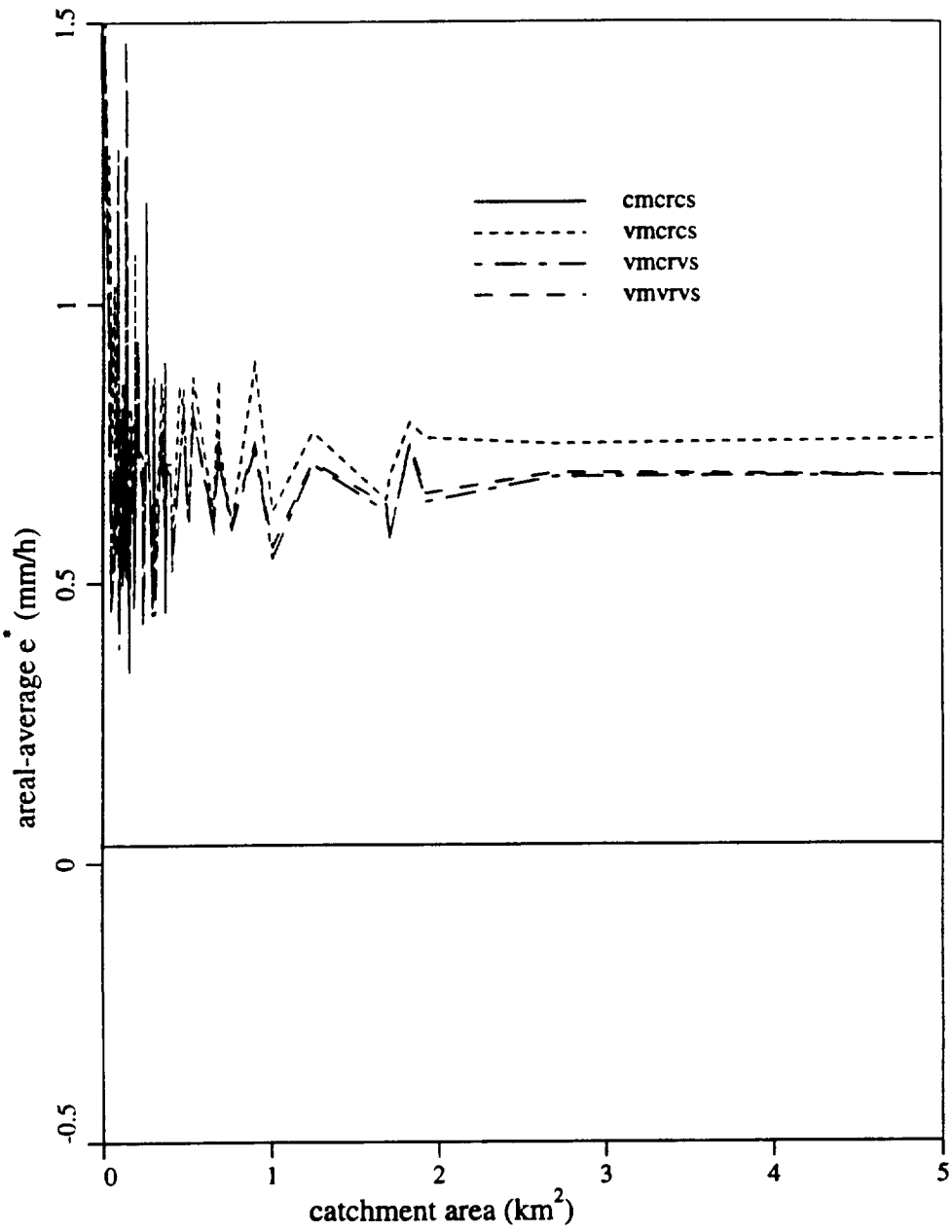

Figure 9. Computed catchment-average exfiltration capacity versus catchment area at 1815 GMT, October 7, 1987 for the following combinations of model inputs: spatially-constant soil moisture, solar radiation, and soil properties (cmcrcs); spatially-variable soil moisture and spatially-constant solar radiation and soil properties (vmcrcs); spatially-variable soil moisture and soil properties and spatially-constant solar radiation (vmcrvs); spatially-variable soil moisture, solar radiation and soil properties (vmvrvs).

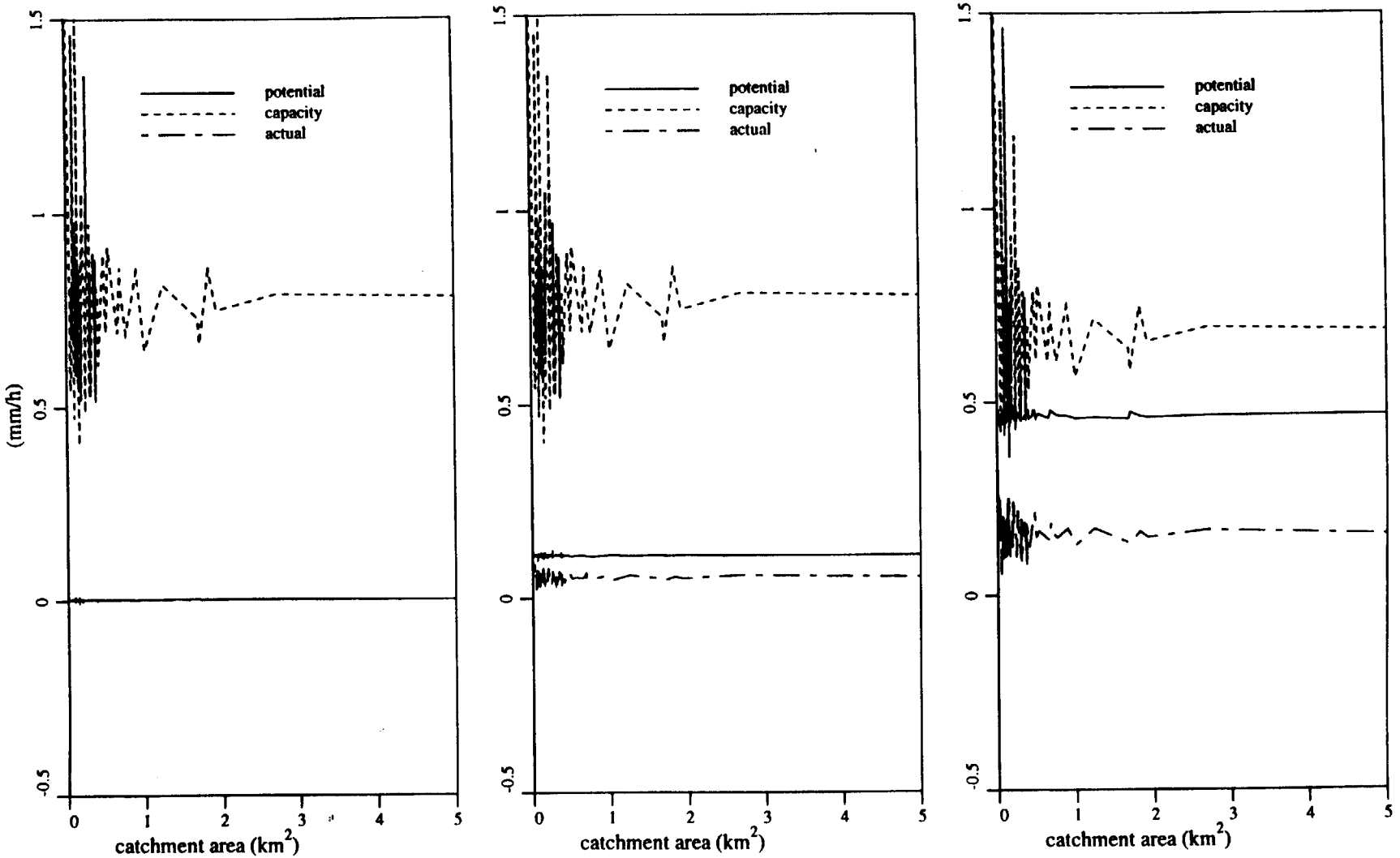
potential
capacity
actual
(mm/h)
1.5
1
0.5
0
-0.5
0
1
2
3
4
5
catchment area (km^2)

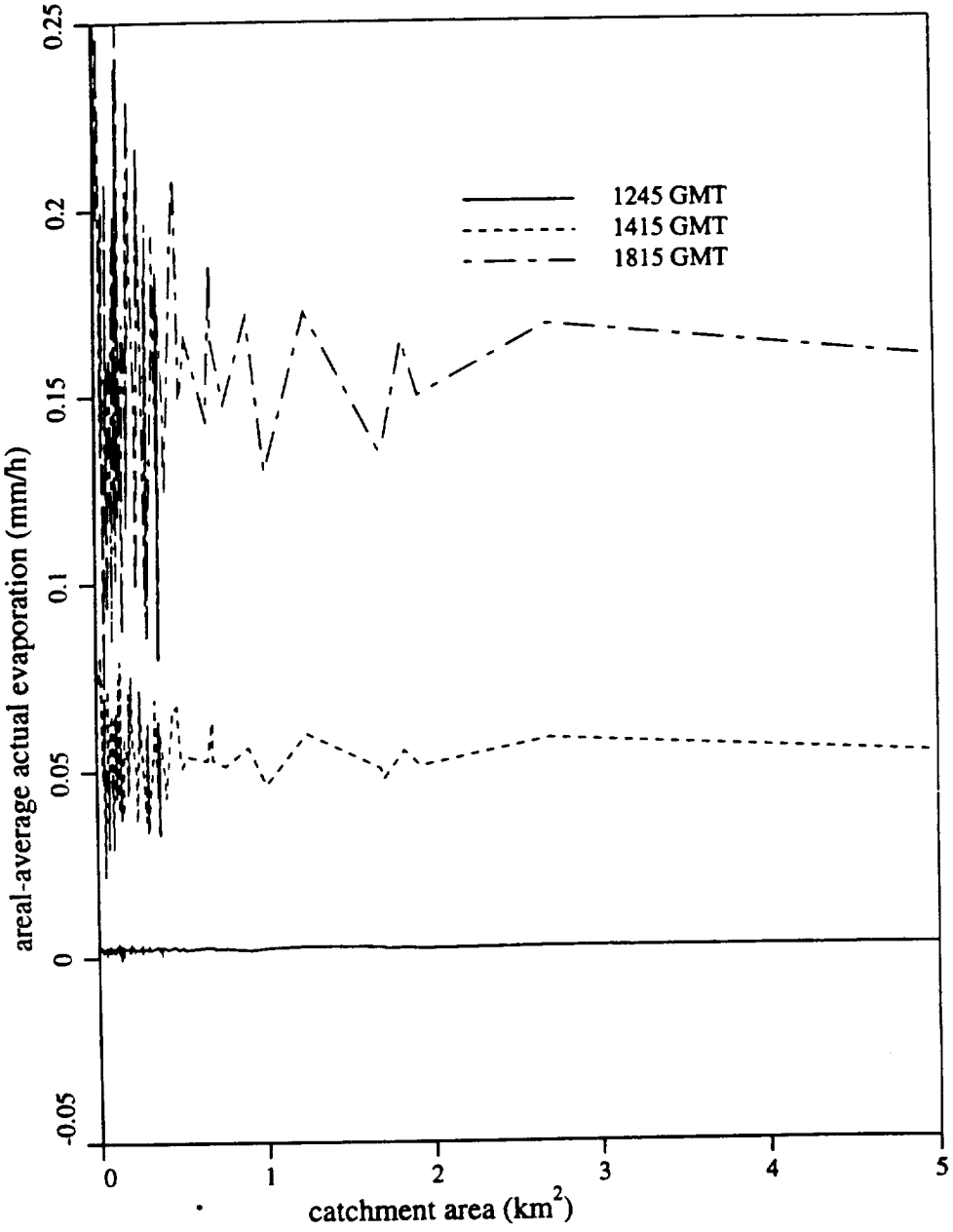

Figure 11. Computed catchment-average actual evaporation rate versus catchment area for 1245, 1415, and 1815 GMT, October 7, 1987.

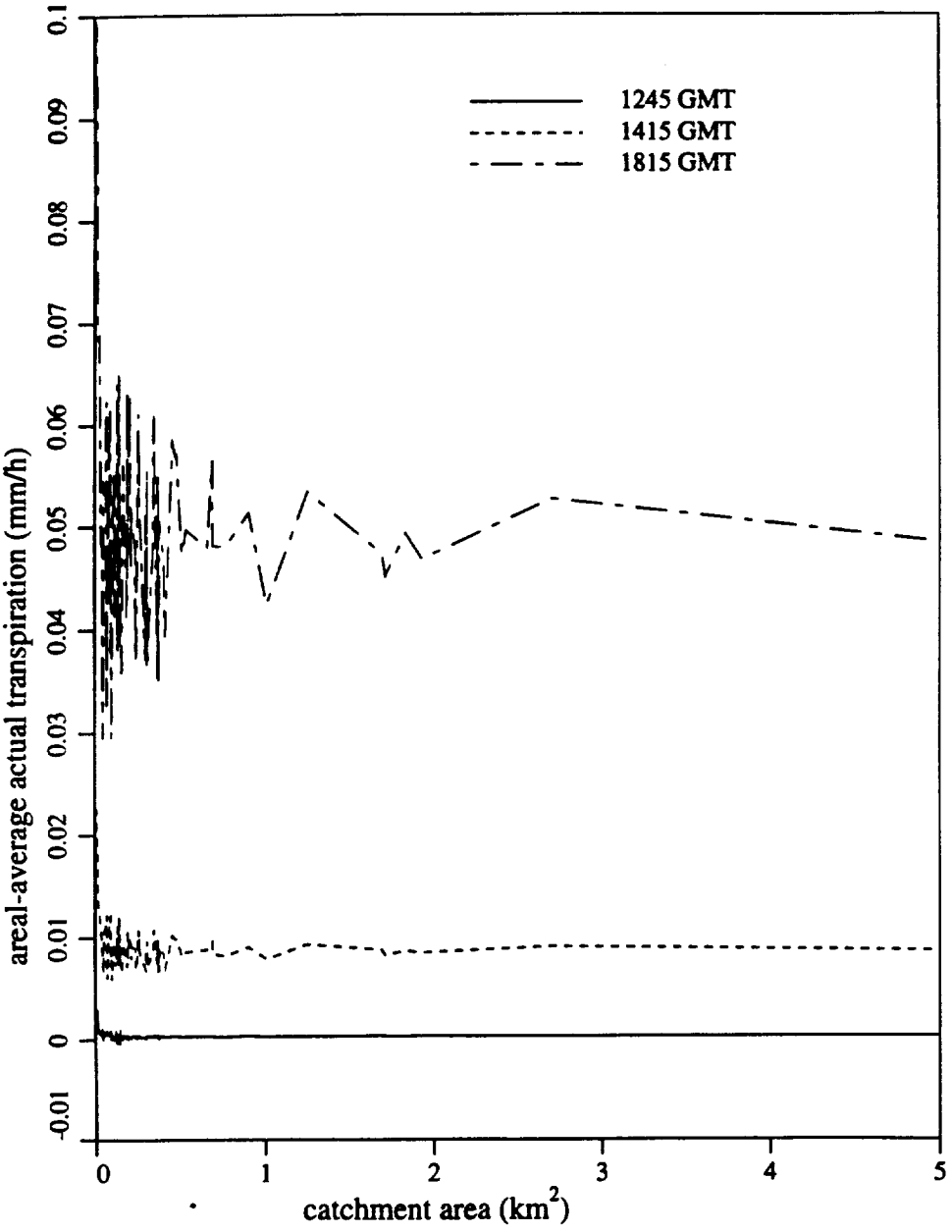

Figure 12. Computed catchment-average actual transpiration rate versus catchment area for 1245, 1415, and 1815 GMT, October 7, 1987.

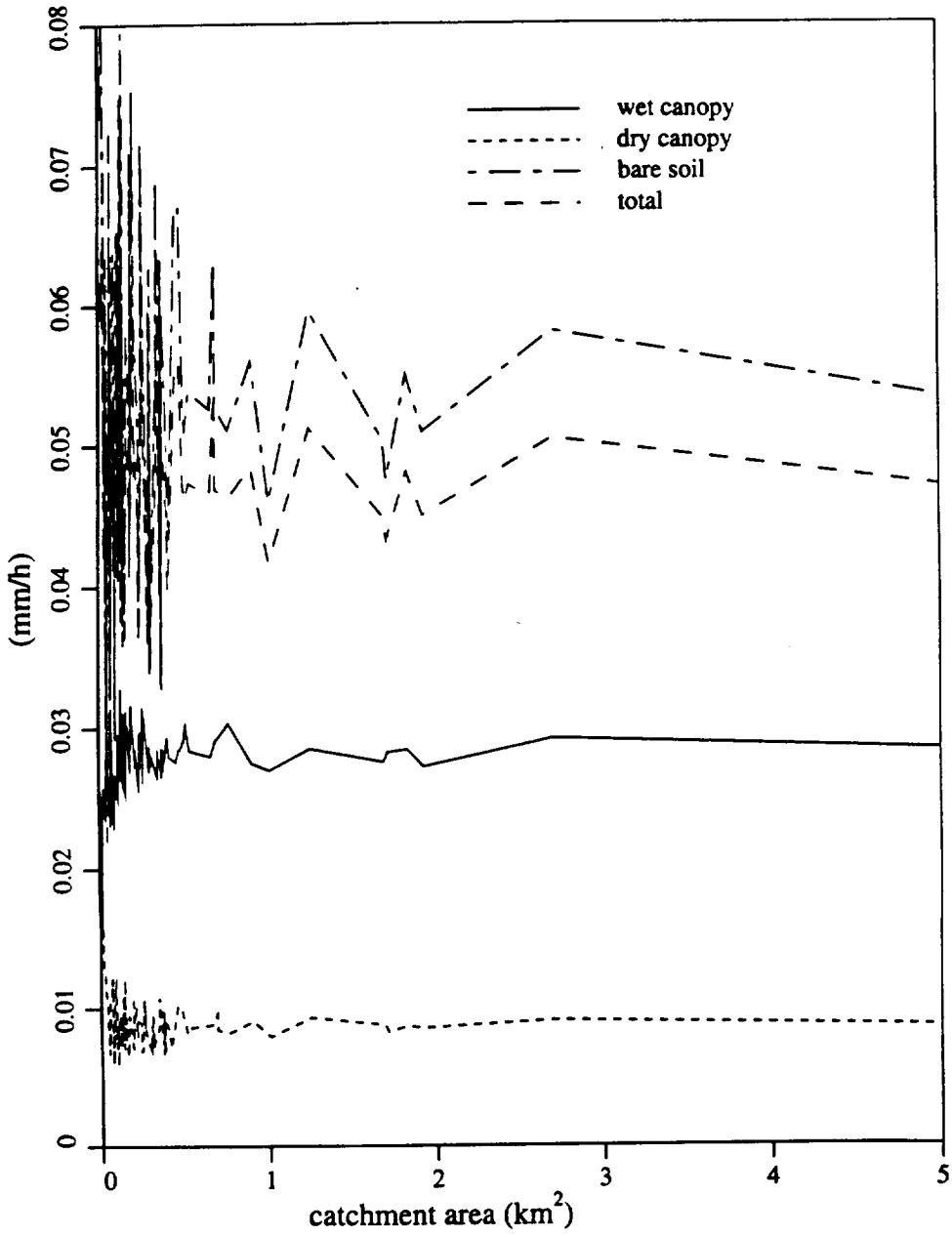

Figure 13. Computed catchment-average evapotranspiration rate, catchment-average wet canopy evaporation rate, catchment-average dry canopy transpiration rate, and catchment-average bare soil evaporation rate versus catchment area for 1415 GMT, October 7, 1987.

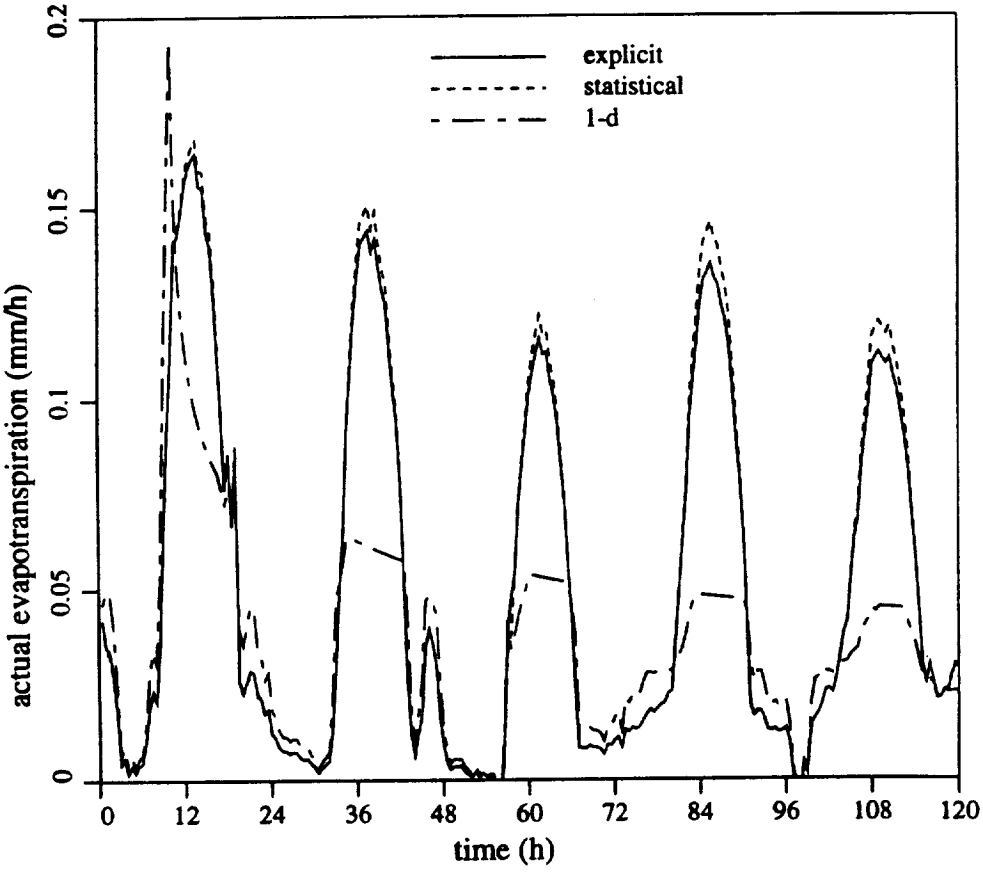

Figure 14. Computed catchment-average evapotranspiration using the spatially-distributed model, the statistically-aggregated model, and the one-dimensional local model, October 5-9, 1987.